Model-free fault detection: application to Polymer Electrolyte Fuel Cell system

Meziane Ait Ziane[1,2] Nadia Yousfi Steiner[1] Cédric Join [3] Michel Benne [2] Cédric Damour [2] Marie Cécile Péra [1]

***Abstract*— A novel fault detection method is presented in this paper. The proposed method can be considered as an extension of the model-free control which is based on an ultra-local model. The model-free controller has demonstrated a great ability to perform the control tasks despite the presence of a fault. This undeniable advantage can mask the effect of a fault resulting in an abnormal degradation impacting one of the components ensuring the control loop or the system itself. The proposed method allows coping with this type of event rapid coping. The basic idea of the diagnostic method is to reconstruct the measured output of the system from the ultra-local model used for system control. The estimated output is compared with the measured one to generate a residual which is employed as the fault indicator. An experimental validation of the polymer electrolyte membrane fuel cell (PEMFC) system is carried out in real time to detect a a system fault that results in membrane flooding. The main advantage of the method is to be able to simultaneously control the system and detect faults that may affect it without needing an accurate knowledge of the mathematical/physical system model. The results obtained are very promising for real-time diagnosis of the polymer electrolyte membrane fuel cell systems.**

I. INTRODUCTION

Proton-exchange membrane fuel cell (PEMFC) is one of the promising technology in the chain of green energy production. The opportunity to produce green hydrogen is driving the use of PEM fuel cells in several applications, whether mobile or stationary [1]. The operating principle of the fuel cell is as follows: at the anode, the hydrogen fuel is oxidized, releasing electrons and protons. The former feeds a charge through an external circuit while the latter pass through the proton exchange membrane located between the electrodes to the cathode, where they are combined with the dissolved oxidant oxygen to produce energy. The fuel cell converts chemical energy of the reactants to produce electricity, water and heat. The coupling between electrical, thermal and chemical aspects qualifies the fuel cell as a complex system. The control and the monitoring of several operating parameters are necessary to maintain high efficiency and avoid system degradation. In [2] the authors identified four crucial operating parameters that have a significant influence on the overall behavior of the PEMFC: gas flow rate, temperature, relative humidity and inlet gas pressure.

Gas flow rate has a direct impact on electrochemical reactions and water management in PEM fuel cells. Insufficient oxygen and hydrogen flow rates result in a drop in PEMFC voltage and can induce a starvation fault [3]. High gas flow can reduce the overall system efficiency and drain water produced within the stack, which can lead to a membrane drying fault. Improper control of inlet gas temperature and humidity directly affects the water content of the membrane and electrodes. Water instability in the membrane and electrodes between incoming, remaining and outgoing water can induce a water management fault. The most common faults related to water management are flooding and drying, their impact is significant on the performance and lifetime of PEMFCs [4]. This is why an appropriate control of the inlet partial pressure is essential to ensure the highest performance and to avoid mechanical degradation of the membrane resulting from the high pressure drop between the cathode and anode sides [5] [6].

Membrane flooding is the most frequent fault encountered during PEMFC operation. Authors in [7] define flooding as an accumulation of excess water in the channels that supply gas to the cell or inside the PEM fuel cell. In the literature, due to its frequent occurrence and significant impact on fuel cell performance, several works dealing with flooding diagnosis can be found. Authors in [8] have constructed a 3D PEMFC model that estimates the temperature, voltage and current of the fuel cell. The constructed model is combined with neural networks to detect and isolate membrane flooding and drying faults. The method is mainly based on the classification of experimental test data under different operating conditions of the PEMFC. In [9] authors suggest an online diagnosis based on a fast electromechanical impedance spectroscopy. Experimental validation on a 3 KW stack shows the effectiveness of detecting the flooding fault and other faults such as drying and starvation. However, a learning step is required before online implementation and the overall system efficiency may decrease, as the hardware used for this method consumes energy. In [10], a signal-based approach is presented. The method is based on a discrete wavelet transform applied to the fuel cell voltage signal. The experimental test on a 500W fuel cell reveals that the flooding fault was successfully detected only by processing the voltage signal. The same signal is assumed in [11] using an empirical mode decomposition technique to detect and

*This work was not supported by any organization

[1] FEMTO-ST instiute, FCLAB, Université Bourgogne Franche-Comte,CNRS, rue Thierry-Mieg, Belfort, 90010, Fraance

[2] ENERGY Lab, Université de La Reunion, rue cassin, Saint-Denis, 97715, France meziane.ait-ziane@univ-reunion.fr

[3] CRAN,(CNRS,UMR 7039), Université de Lorraine BP 239, Vandoeuvre-les-Nancy, 54506, Fraance

isolate the flooding and drying fault. The method is applied online on a single cell of 50W power.

Moreover, in [12] authors indicate that the pressure difference on the cathode side is an excellent indicator of flooding. In [13] a model-based diagnosis related to pressure drop is proposed. A neural network is employed, the validation of the model is done by off-line training data from a normal operation. Fault detection is achieved by generating two residuals, the first one is used to check the consistency between the measured cathode pressure drop and the one computed by the neural network model. The second residual is generated by the comparison of the PEMFC voltage signals. Flooding is detected and isolated when both residuals exceed the defined threshold. As membrane drying has no effect on the cathodic pressure drop, the evolving voltage residual and a stable pressure residual is the symptom of a drying situation. In fact, several works that deal with cathodic pressure drop flooding fault detection are presented in [14]. The authors report that few methods have been tested online to detect flooding using pressure drops.

Model-based diagnostic approaches are not widely applied for real-time applications. This may be due to the fact that a model which accurately describes the PEMFC is difficult to achieve. For this reason, these methods are usually evaluated through simulation. Signal processing based approaches are appropriate for these applications, but generally require certain conditions such as signal stationarity and the choice of the signal analysis window that influences the diagnostic accuracy [11].

In order to overcome these obstacles, a new fault detection method is presented in this paper. The proposed diagnostic method is derived from model-free control or *iPID* [15], which has the advantage of controlling complex systems in which the precise physical/mathematical model is not necessarily known in its entirety [16]. The global model of the system is replaced by an ultra-local model used to design the control law. In addition, the low computational cost and the ease of online implementation are major advantages of the proposed fault detection and control strategy. The developed fault detection method is essentially based on the reconstruction of the system output from the ultra-local model. The reconstructed output is considered as an estimate of the measured one. A residual signal is generated to check the consistency between the measured and the estimated output in order to detect the fault. Since the overall strategy of the proposed method provides both control and fault detection, it is appropriate to control the inlet pressure difference of the PEMFC system in order to avoid the mechanical degradation of the membrane. Concurrently, the detection of flooding is provided in real-time. The global strategy is validated on a stack of 1.2KW power.

This paper is organized as follows: the presentation of the model-free control and fault detection method with an illustration of the detection of an actuator fault on a linear and non linear system are shown in the second section. The real-time application of the proposed method on the fuel cell system is illustrated in third section. Conclusion is given in the fourth section.

II. Model free control and model free fault detection

First, a brief presentation of the model-free controller is given in the following.

A. Model free controller

The main idea of the model-free controller is to replace the global mathematical model that represents the behaviour of the system by an ultra-local model [17], which is expressed as follows:

$$y^{(\nu)}(t) = F(t) + \alpha.u(t) \tag{1}$$

Where: ν is the order of derivation of the output y, u is the input of the system, α is a parameter set by the user and F is a function that gathers all the unknown part of the system that is estimated from the measured output y and the calculated input u.

The authors in [18] propose an algebraic method for estimating the function F that is robust to noise, in the event of $\nu = 1$, the estimated function $\hat{F}$ is given by:

$$\hat{F}(t) = \frac{-3!}{T^3}\int_{t-T}^{t}(T-2t)y(t) + \alpha t(T-t)u(t)\mathrm{d}t \tag{2}$$

Where $T > 0$ might be small and $[t-T;t]$ denotes the sliding windows of the integration interval. When ν is taken 1 which is the case in this paper, the designed controller is referred to as *iP* controller, the closed loop control is given as follows:

$$u(t) = \frac{1}{\alpha}\left(-\hat{F}(t) + \dot{y}_d(t) + k_p e(t)\right) \tag{3}$$

Where :

- y_d is the desired trajectory.
- $e = y_d - y$ is the tracking error.
- k_p is the tuning gain of the proportional controller.

B. Model free fault detection

The basic idea of the developed method is to reconstruct the output of the system from the ultra-local model given by (1). As the input u and the function $\hat{F}$ are calculated for the control of the system, the estimation of y can be performed.

Consider that $\nu = 1$, based on the ultra-local model given in (1), the output y is expressed as follows:

$$y(t) = \int_0^t \left(F(\tau) + \alpha u(\tau)\right)d\tau + y(0) \tag{4}$$

Where $y(0)$ is an initial condition of the output. In a practical case, the estimate of F is not exact, this is mainly due to computational considerations, but also the noise that affects the measured output. The estimation error can be expressed as:

$$\hat{F}(t) = F(t) - \Delta F(t) \tag{5}$$

By substituting (5) in (4), it is obtained:

$$y(t) = \int_0^t \left(\hat{F}(\tau) + \alpha u(\tau) + \Delta F(\tau)\right)d\tau + y(0) \tag{6}$$

In practice, the calculated $\hat{y}$ is given by:

$$\hat{y}(t) = \int_0^t \left(\hat{F}(\tau) + \alpha u(\tau)\right) d\tau + \hat{y}(0) \tag{7}$$

The initial conditions are taken to be $\hat{y}(0) \neq 0$ and $y(0) \neq 0$. Supposing that the estimation error is zero $\Delta F(t) = 0$ and $\hat{y}(0) = y(0)$, it results in $\hat{y}(t) = y(t)$, even in the presence of fault and/or disturbance, the fault is then undetectable. However, the estimation error is never zero ($\Delta F(t) \neq 0$) for the practical case and $\hat{y}(t) \neq y(t)$ even in the absence of fault.

In order to correct the estimation error and to generate a zero residual signal in the absence of fault/disturbance, a parameter β is introduced on $\hat{y}$. The residual signal that is employed as a fault indicator is given by:

$$r(t) = y(t) - \beta\hat{y}(t) \tag{8}$$

Where β is constant parameter for all linear systems and nonlinear systems that have a linear static characteristic. For the remaining systems, β is the value of $\beta(t)$ in steady state. The expression of $\beta(t)$ is given as follows:

$$\beta(t) = \frac{y(t)}{\hat{y}(t)} = \frac{y(t)}{\int_0^t \left(\hat{F}(\tau) + \alpha u(\tau)\right) d\tau + \hat{y}(0)} \tag{9}$$

Once β is determined, the residual of (8) is zero in the absence of fault and disturbance. The manifestation of the latter causes an abnormal change in the output y, and as the controller *iP* tolerates the fault the output y is brought back to the desired value but $\beta\hat{y}$ diverges from the measured y. The authors of [19] illustrate by simulation the proposed method for actuator fault detection on linear and nonlinear systems. In this paper an experimental validation is performed in order to validate the feasibility of the real-time implementation of the proposed method. It is important to mention that with the proposed fault detection method, the initial condition is assumed to be approximately known $\hat{y}(0) \simeq y(0)$. There is no differentiation between an actuator fault and a disturbance, any residual deviation is interpreted as a fault.

III. Validation of Model-Free Fault Detection

A. Simulation part

In order to illustrate the crucial role of β in the correction of the reconstructed output and to investigate its behavior, a case study on a linear and nonlinear system is first performed by simulation.

1) Linear system: Consider a linear system described by the following transfer function:

$$\frac{y(s)}{u(s)} = \frac{(s+2)^2}{(s+2.2)^3} \tag{10}$$

An *iP* controller is employed, with $k_p = 10$, $\alpha = 0.6$ and $T_e = 0.001$. Fig.1 shows that the trajectory tracking is well respected with the *iP* controller. However, the estimated output computed by (7) never corresponds to the measured one as shown in Fig.1. For this reason, a correction by the β parameter must be performed to correct the estimated output. The evolution of the latter is presented in Fig.2, where $\beta(t)$ is calculated by (9). It is clearly shown that this parameter

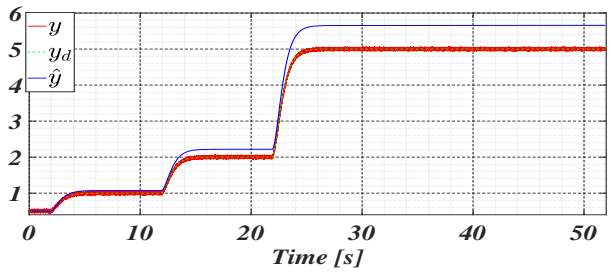

Fig. 1: Trajectory tracking : y and $\hat{y}$, fault free case

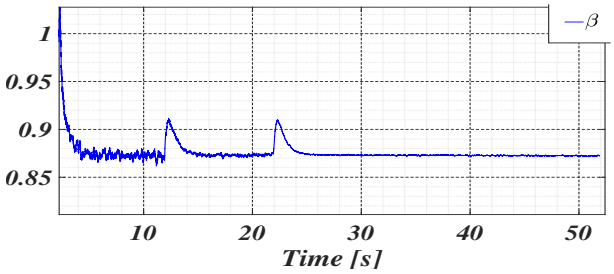

Fig. 2: Evolution of β in fault free case

always converges to a constant value despite the variations of the trajectory with different amplitudes. The retained value of β that is used to correct the estimated output in order to obtain a zero residual in the absence of actuator fault is 0.873, which corresponds to the value of $\beta(t)$ in steady state.

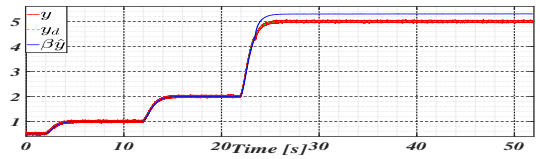

(a) Trajectory tracking :y and $\beta\hat{y}$ actuator fault

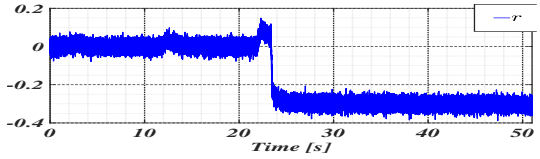

(b) Residue

Fig. 3: Linear system actuator fault

Fig.3(a) shows the estimated corrected output with a constant β. It is clearly shown that $\beta\hat{y}$ follows perfectly the measured output y during the first two setpoint changes. A power loss actuator fault with $u_f = 0.7.u$ is simulated at $t = 22.4s$ in transient regime, when the fault occurs $\beta\hat{y}$ immediately diverges from y. During the first two setpoint changes, small fluctuations are observed on the residual. Nevertheless, it always returns to its initial position which is 0 in the absence of a fault, see Fig.3(b). Once the fault is manifested, the residual diverges and never returns to 0, which allows the detection of the actuator fault. For systems with linear static characteristics, the parameter β is determined at the first change of trajectory and remains constant for the other setpoint changes.

2) Nonlinear system: Consider a nonlinear system expressed as follows:

$$\dot{y} = y + u^3.f \tag{11}$$

The parameter of the *iP* controller are: $k_p = 10$, $\alpha = 4$ and $T_e = 0.001$. Where d refers to presence of actuator fault when $f < 1$, no fault is considered when $f = 1$. The purpose is to investigate the behavior of β during setpoint changes for this system.

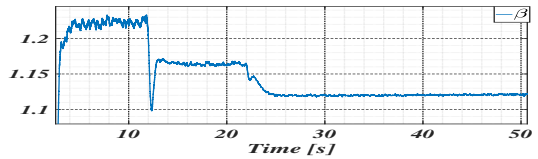

(a) Evolution of $\beta(t)$: fault free case

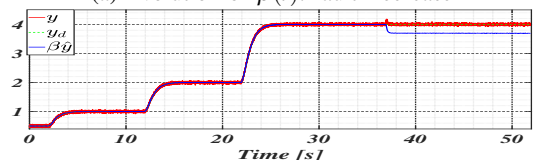

(b) y and $\beta\hat{y}$: actuator fault

Fig. 4: Non-linear system actuator fault

Fig.4(a) shows that the parameter β evolves according to the setpoint changes and never converges to the same value, in fault free case. This parameter must be recalculated for each new setpoint changes to correct the estimated output $\hat{y}$. However, this allows the actuator fault/disturbance to be detected only in steady state. The actuator fault is simulated with $f = 0.7$ at $t = 37s$, as shown in Fig.4(b). The occurrence of the fault results in a discrepancy of $\beta\hat{y}$ with respect to y. This enables the detection of actuator fault. For systems where $\beta(t)$ evolves with setpoint changes, β must be updated for each setpoint change, see [19].

B. Experimental validation: application to PEMFC system

An experimental validation is performed on a PEM fuel cell system of 1.2KW power. The objective of this application is twofold: control the inlet pressure difference to avoid membrane degradation and detect the flooding which is considered as a system fault. The authors in [5] show that the model-free control provides half the inlet pressure difference compared to the industrial PID controller, for the identical fuel cell type. The PEMF fuel cell on which the test is performed is a stack with 12 cells having an active area of $90cm^2$. This stack is installed in a test bench able to operate stacks of a power up to 1.5KW. More details on the design of the test bench are available in [5]. The control of the PEMFC inlet pressure can be achieved by acting on the back pressure valve located at the gas outlet. The opening and closing of the back pressure valves which ensure the control of the inlet pressure is provided by a signal [4-20mA]. This signal is sent directly by the *iP* controllers which are implemented in Labview where all signals are acquired with a frequency of 3Hz. The measurement of all PEMFC parameters is available (stack temperature, voltage, relative humidity of incoming gases, gas flow, inlet and outlet pressure).

Two *iP* controllers are employed to act on each back pressure valve. The main objective is to maintain the inlet gas pressure difference around 0. The estimation of the inlet cathode pressure is performed and employed for flooding detection. The overall strategy for inlet pressure difference control and flooding fault detection is illustrated in Fig.5.

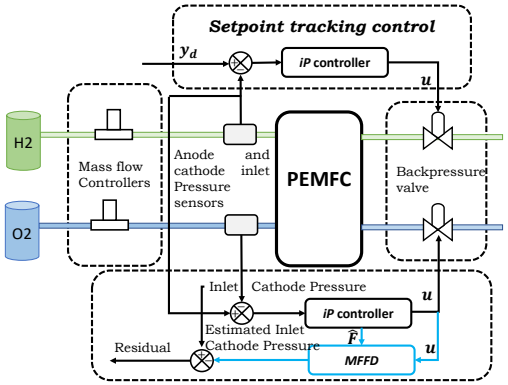

Fig. 5: Model-free fault detection and *iP* controller applied to PEMFC system

The closed loop control for the hydrogen inlet pressure is given by:

$$u_a(t) = \frac{1}{0.7}\left(-\hat{F}_a(t) + \dot{y}_d(t) + 3e_a(t)\right) \tag{12}$$

Where: $e_a = y_d - P_a$, and P_a is the inlet hydrogen pressure. The closed loop for the cathode side is given by:

$$u_c(t) = \frac{1}{0.4}\left(-\hat{F}_c(t) + \dot{P}_a(t) + 5e_c(t)\right) \tag{13}$$

Where: $e_c = P_a - P_c$, and P_c is the inlet air pressure. The estimated inlet pressure is calculated by:

$$\hat{P}_c(t) = \int_0^t \left(\hat{F}_c(\tau) + 5u_c(\tau)\right) d\tau + \hat{P}_c(0) \tag{14}$$

Where: $\hat{P}_c(0) \simeq P_c(0)$. The residual that is employed for flooding detection is expressed as:

$$r(t) = P_c(t) - \beta\hat{P}_c(t) \tag{15}$$

Where β is the value of $\beta(t)$ in steady state. Since the dynamics of the PEMFC are highly nonlinear, β must be adjusted for each new setpoint change to obtain a zero residual in the absence of a fault and/or disturbance. Table I shows the PEM fuel cell operating conditions for this experiment.

TABLE I: PEMFC operating conditions

Parameter	Value
Current	49 A
Air stoichiometry λ_{Air}	2
Hydrogen stoichiometry λ_{H2}	2
Hydrogen *RH*	64%

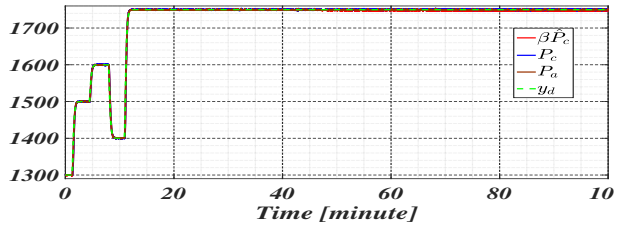

Fig. 6: Inlet pressure trajectory tracking with cathodic inlet pressure estimation: flooding fault

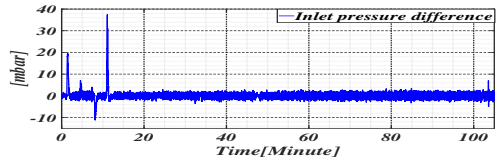

(a) Inlet pressure difference

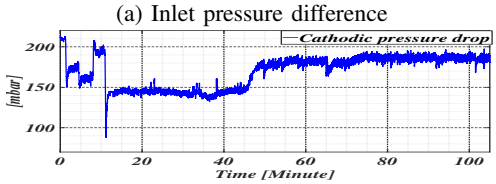

(b) Cathodic pressure drop

Fig. 7: Cathodic pressure: PEMFC system

The total duration of the experiment is 105 minutes, the first 13 minutes are devoted to varying the inlet pressure to evaluate the performances of the controllers to reduce the inlet pressure difference and to investigate the behavior of β. Fig.6 reveals that the tracking of the trajectory is always achieved, i.e., the anode inlet pressure perfectly follows the desired trajectory and the cathode inlet pressure accompanies the anode inlet pressure. This results in a slightly varying pressure difference around 0 as shown in Fig.7(a). The largest pressure difference recorded for the four setpoint changes is 40 mbar. This is a very satisfactory result, as the limit of the pressure difference set by the stack manufacturer is 300 mbar. Increasing the gas inlet pressure contributes significantly to the improvement of the PEMFC performance, as shown in Fig.8, the voltage signal increases with increments in the inlet pressure.

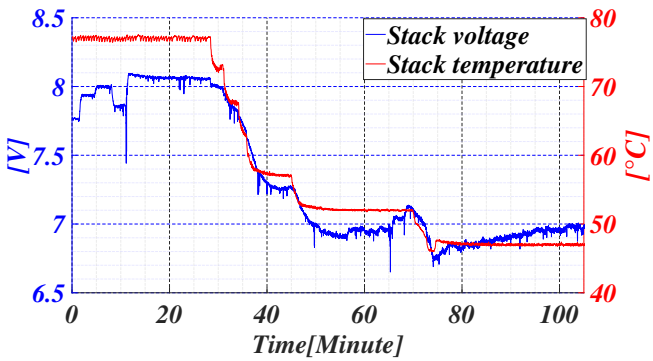

Fig. 8: Stack voltage and temperature

The temperature of the PEMFC is regulated around 75°C, which corresponds to normal operation. Once all operating conditions are stabilized around their operating point, i.e. the inlet pressure is 1750 mbar, β corresponding to this operating point is determined and the voltage signal is also stable. The stack temperature is gradually decreased, as shown in Fig.8.

The purpose of these progressive temperature decreases is to illustrate the impact of temperature changes on the stack performances and on the occurrence of flooding fault. It can be seen that the stack voltage decreases as the temperature drops. Once the temperature is stabilized, the stack voltage also stabilizes, indicating the [38-45min] interval. However, the estimated cathode inlet pressure always remains stable and similar to the set point and measured inlet air pressure, meaning that there is no disturbance on the cathode pressure, as visible in Fig.9. Another temperature change up to 52°C is performed in the interval [46-70min].

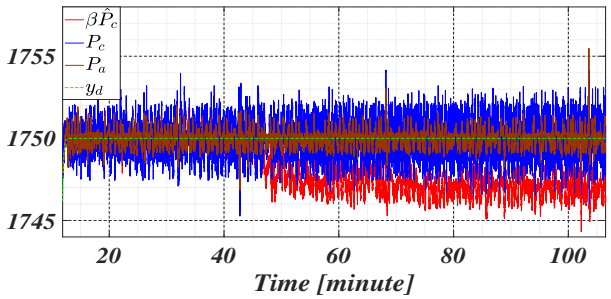

Fig. 9: Measured and estimated cathode inlet pressure

The estimated cathodic inlet pressure starts to diverge from 48min, which means that a disturbance on the cathodic inlet pressure is in progress, as shown in the Fig.9. This disturbance corresponds to the condensation of water in the stack which has an impact on the cathodic pressure. The cathode inlet pressure tends to increase when water condensation occurs in the stack. However, as the *iP* Controller tolerates disturbances, it remains at the desired value. Once this disturbance is occurring, the proposed fault detection method easily detects it.

The residual signal that is used as an indicator of the flooding fault is shown in Fig.10(b). Since the cathode inlet pressure measurement is noisy, the residual signal is also noisy. In order to facilitate the analysis of this signal without fault detection false alarms, *cusum* algorithm is introduced to evaluate the evolution of the residual signal [20]. The calculation of *cusum* is performed as follows:

- Calculation of the mean m_0 of the first samples of r.
- Initialization of $cusum(1) = r(1) - m_0$.
- Calculation of the mean $m(t)$ of r in a sliding interval $[t-h,t]$, where h is the size of the sliding window.
- Calculation of $cusum(t) = cusum(t-1) + r(t) - m(t)$.

The flooding fault is detected from the 48min, i.e. when the cusum residual exceeds the defined threshold and remains stable for the rest of the test. The threshold is determined empirically according to the evolution of the cumulative sum of residue in normal operation. The evolution of the residual

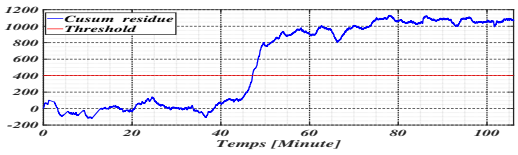

(a) CUSUM of residue

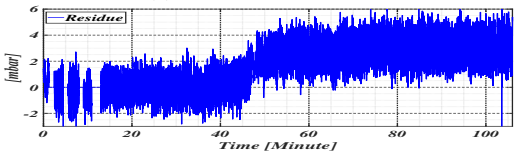

(b) Residue

Fig. 10: Flooding detection

signal is related to the fact that the estimated inlet pressure is different from the measured inlet pressure. The latter diverges due to the fact that the inlet pressure of the stack tries to increase. Fig.7(b) shows that the cathodic pressure drop increases as the estimated pressure diverges. This confirms that flooding has occurred at this time.

The proposed diagnosis tool allows the real-time detecting of the water condensation fault in the stack.

IV. CONCLUSIONS

A real-time validation of model-free fault detection is presented in this paper. Flooding fault detection is achieved without any specific knowledge of the fuel cell model. Additionally, the inlet pressure difference is controlled and maintained around 0, which prevents mechanical degradation of the membrane. In the literature, only few methods can provide simultaneously real-time fault detection and control of the inlet pressure, which is the main advantage of the proposed method for PEMFC diagnosis. However, some improvements are needed in the fault detection method to be able to detect the fault in transient state for strongly nonlinear systems. Since the PEMFC operates under stable operating conditions (i.e., there is no excessive change in setpoints), the proposed method is considered an important advance in the real-time diagnosis of this system.

ACKNOWLEDGMENT

The Virtual-FCS project has received funding from the Fuel Cells and Hydrogen 2 Joint Undertaking (now Clean Hydrogen Partnership) under Grant Agreement No 875087. This Joint Undertaking receives support from the European Union's Horizon 2020 research and innovation programme, Hydrogen Europe and Hydrogen Europe Research. This work has been supported by the EIPHI Graduate school (contract "ANR-17-EURE-0002").

REFERENCES

[1] J. Aubry, N. Y. Steiner, S. Morando, N. Zerhouni, and D. Hissel, "Fuel cell diagnosis methods for embedded automotive applications," *Energy Reports*, vol. 8, pp. 6687–6706, 2022.

[2] H. Askaripour, "Effect of operating conditions on the performance of a PEM fuel cell," *International Journal of Heat and Mass Transfer*, vol. 144, p. 118705, Dec. 2019. [Online]. Available: https://linkinghub.elsevier.com/retrieve/pii/S0017931019328467

[3] E. Pahon, D. Hissel, S. Jemei, and N. Y. Steiner, "Signal-based diagnostic approach to enhance fuel cell durability," *Journal of Power Sources*, vol. 506, p. 230223, 2021.

[4] E. Dijoux, N. Y. Steiner, M. Benne, M.-C. Péra, and B. Grondin-Perez, "Fault structural analysis applied to proton exchange membrane fuel cell water management issues," *Electrochem*, vol. 2, no. 4, pp. 604–630, 2021.

[5] M. Ait Ziane, M. Pera, C. Join, M. Benne, J. Chabriat, N. Y. Steiner, and C. Damour, "On-line implementation of model free controller for oxygen stoichiometry and pressure difference control of polymer electrolyte fuel cell," *International Journal of Hydrogen Energy*, 2022.

[6] C. Lin-Kwong-Chon, C. Damour, M. Benne, J.-J. A. Kadjo, and B. Grondin-Pérez, "Adaptive neural control of pemfc system based on data-driven and reinforcement learning approaches," *Control Engineering Practice*, vol. 120, p. 105022, 2022.

[7] W. Schmittinger and A. Vahidi, "A review of the main parameters influencing long-term performance and durability of pem fuel cells," *Journal of power sources*, vol. 180, no. 1, pp. 1–14, 2008.

[8] A. Mohammadi, A. Djerdir, N. Y. Steiner, and D. Khaburi, "Advanced diagnosis based on temperature and current density distributions in a single pemfc," *International Journal of Hydrogen Energy*, vol. 40, no. 45, pp. 15 845–15 855, 2015.

[9] H. Lu, J. Chen, C. Yan, and H. Liu, "On-line fault diagnosis for proton exchange membrane fuel cells based on a fast electrochemical impedance spectroscopy measurement," *Journal of Power Sources*, vol. 430, pp. 233–243, 2019.

[10] N. Y. Steiner, D. Hissel, P. Moçotéguy, and D. Candusso, "Non intrusive diagnosis of polymer electrolyte fuel cells by wavelet packet transform," *International Journal of Hydrogen Energy*, vol. 36, no. 1, pp. 740–746, 2011.

[11] C. Damour, M. Benne, B. Grondin-Perez, M. Bessafi, D. Hissel, and J.-P. Chabriat, "Polymer electrolyte membrane fuel cell fault diagnosis based on empirical mode decomposition," *Journal of Power Sources*, vol. 299, pp. 596–603, 2015.

[12] G. Dotelli, R. Ferrero, P. G. Stampino, S. Latorrata, and S. Toscani, "Combining electrical and pressure measurements for early flooding detection in a pem fuel cell," *IEEE Transactions on Instrumentation and Measurement*, vol. 65, no. 5, pp. 1007–1014, 2015.

[13] N. Y. Steiner, D. Hissel, P. Moçotéguy, and D. Candusso, "Diagnosis of polymer electrolyte fuel cells failure modes (flooding & drying out) by neural networks modeling," *International journal of hydrogen energy*, vol. 36, no. 4, pp. 3067–3075, 2011.

[14] P. Pei, Y. Li, H. Xu, and Z. Wu, "A review on water fault diagnosis of pemfc associated with the pressure drop," *Applied Energy*, vol. 173, pp. 366–385, 2016.

[15] M. Fliess and C. Join, "Model-free control," *International Journal of Control*, vol. 86, no. 12, pp. 2228–2252, 2013.

[16] L. Michel, I. Neunaber, R. Mishra, C. Braud, F. Plestan, J.-P. Barbot, X. Boucher, C. Join, and M. Fliess, "Model-free control of the dynamic lift of a wind turbine blade section: experimental results," in *Journal of Physics: Conference Series*, vol. 2265, no. 3. IOP Publishing, 2022, p. 032068.

[17] M. Fliess and C. Join, "An alternative to proportional-integral and proportional-integral-derivative regulators: Intelligent proportional-derivative regulators," *International Journal of Robust and Nonlinear Control*, 2021.

[18] M. Fliess and H. Sira-Ramirez, "Closed-loop parametric identification for continuous-time linear systems via new algebraic techniques," in *Identification of Continuous-time Models from sampled Data*. Springer, 2008, pp. 363–391.

[19] M. Ait Ziane, C. Join, M.-C. Pera, N. Y. Steiner, M. Benne, and C. Damour, "A new method for fault detection in a free model context," *IFAC-PapersOnLine*, vol. 55, no. 6, pp. 55–60, 2022.

[20] M. Basseville, I. V. Nikiforov *et al.*, *Detection of abrupt changes: theory and application*. prentice Hall Englewood Cliffs, 1993, vol. 104.